

Comb-assisted subkilohertz linewidth quantum cascade laser for high-precision mid-infrared spectroscopy

I. Galli, M. Siciliani de Cumis, F. Cappelli, S. Bartalini, D. Mazzotti et al.

Citation: *Appl. Phys. Lett.* **102**, 121117 (2013); doi: 10.1063/1.4799284

View online: <http://dx.doi.org/10.1063/1.4799284>

View Table of Contents: <http://apl.aip.org/resource/1/APPLAB/v102/i12>

Published by the [American Institute of Physics](http://www.aip.org).

Additional information on *Appl. Phys. Lett.*

Journal Homepage: <http://apl.aip.org/>

Journal Information: http://apl.aip.org/about/about_the_journal

Top downloads: http://apl.aip.org/features/most_downloaded

Information for Authors: <http://apl.aip.org/authors>

ADVERTISEMENT



Goodfellow
metals • ceramics • polymers • composites
70,000 products
450 different materials
small quantities fast

www.goodfellowusa.com



Comb-assisted subkilohertz linewidth quantum cascade laser for high-precision mid-infrared spectroscopy

I. Galli,^{1,2} M. Siciliani de Cumis,¹ F. Cappelli,^{1,2,a)} S. Bartalini,^{1,2} D. Mazzotti,^{1,2} S. Borri,³ A. Montori,² N. Akikusa,⁴ M. Yamanishi,⁵ G. Giusfredi,^{1,2} P. Cancio,^{1,2} and P. De Natale^{1,2}

¹CNR-INO-Istituto Nazionale di Ottica, Largo E. Fermi 6, 50125 Firenze, FI, Italy

²LENS-European Laboratory for Non-Linear Spectroscopy, Via Carrara 1, 50019 Sesto Fiorentino, FI, Italy

³CNR-IFN-Istituto di Fotonica e Nanotecnologie, Via Amendola 173, 70126 Bari, BA, Italy

⁴Development Bureau Laser Device R&D Group, Hamamatsu Photonics KK, Shizuoka 434-8601, Japan

⁵Central Research Laboratories, Hamamatsu Photonics KK, Shizuoka 434-8601, Japan

(Received 24 December 2012; accepted 19 March 2013; published online 29 March 2013)

We report on the linewidth narrowing of a room-temperature mid-infrared quantum cascade laser by phase-locking to a difference-frequency-generated radiation referenced to an optical frequency comb synthesizer. A locking bandwidth of 250 kHz, with a residual rms phase-noise of 0.56 rad, has been achieved. The laser linewidth is narrowed by more than 2 orders of magnitude below 1 kHz, and its frequency is stabilized with an absolute traceability of 2×10^{-12} . This source has allowed the measurement of the absolute frequency of a CO₂ molecular transition with an uncertainty of about 1 kHz. © 2013 American Institute of Physics. [<http://dx.doi.org/10.1063/1.4799284>]

For longer than a decade, spectroscopy and frequency metrology have been taking advantage of optical frequency comb synthesizers (OFCSs). These devices are able to provide a single-step link between optical and radiofrequency spectral regions.¹ Their extension to the mid-infrared (IR) range² has been based on down-conversion of near-IR OFCSs, achieved either by difference-frequency generation (DFG)^{3–6} or by synchronously pumped optical parametric oscillators (OPOs).^{7,8} When highly stable continuous-wave (CW) mid-IR radiation is required, DFG has proven to be a suitable scheme, obtained by locking visible/near-IR pump and signal lasers to an OFCS and mixing them in a non-linear crystal.⁹ By using more sophisticated schemes, such as intracavity DFG¹⁰ or OPOs,¹¹ it is possible to generate mid-IR radiation with outstanding spectral properties like absolute frequency traceability, becoming suitable for high-sensitivity¹² and high-precision^{13,14} spectroscopy. However, even intracavity DFG-based sources provide, in the best case, few tens of mW power and, as well as OPOs, are based on complex, delicate, and expensive setups. A convenient and robust alternative for power scaling is represented by CW, room-temperature (RT) mid-IR quantum cascade lasers (QCLs),¹⁵ which nowadays provide large tuning capabilities¹⁶ and watt-level powers.¹⁷ While these features make them the ideal sources for a wide range of applications, a crucial step towards their extensive use also for demanding spectroscopic and metrological experiments is the development of techniques for narrowing their emission and for referencing them to a stable frequency standard. Significant advances in the knowledge of the quantum-limited frequency fluctuations of QCLs have been recently made.^{18–21} In particular, the high spectral purity of QCLs has been pointed out, with intrinsic linewidths as low as hundreds of hertz.²⁰ It can be practically accessed only by stabilization techniques, since, in free-running conditions, QCLs show linewidths of the order of

few MHz. Frequency locking of the QCL radiation to a molecular transition²² and optical injection locking using an OFCS-referenced DFG source as master radiation²³ are two possible solutions for linewidth narrowing and absolute frequency referencing of QCLs.

Direct phase-locking of the QCL to an OFCS is a valid alternative, allowing to enhance frequency stability while preserving the full tunability of the laser source.²⁴ Recently, a mid-IR QCL was phase-locked to a 2 μm OFCS by using an up-conversion non-linear process.²⁵ In this case, the final QCL linewidth is limited by the excess phase-noise of the OFCS tooth transferred to it by its reference oscillator. Alternatively, direct phase-locking a QCL to an OFCS-referenced non-linear CW source provides, simultaneously, an absolute frequency reference and a residual phase-noise independent of the OFCS noise. In this paper, we present such scheme with a final QCL narrowing below the OFCS tooth linewidth: indeed, a linewidth below 1 kHz in 1 ms was measured from the analysis of the frequency noise power spectral density (FNPSD). The QCL frequency stability and the absolute traceability have been characterized, resulting both limited by the Rb-GPS (Global Positioning System) disciplined 10-MHz quartz oscillator reference of the OFCS. Precision and high resolution spectroscopy performances of this QCL source are tested by measuring the frequency of the saturation Lamb dip of a CO₂ transition with an uncertainty of 2×10^{-11} .

We used a distributed-feedback QCL emitting at 4.3 μm, provided by Hamamatsu Photonics, from the same processing of the QCL characterized in Ref. 20. It is operated at a temperature of 283 K and a current of 710 mA, delivering an output power of about 5 mW. The radiation in which the QCL has been locked to is produced by non-linear DFG process in a periodically-poled LiNbO₃ crystal by mixing an Yb-fiber-amplified Nd:YAG laser at 1064 nm and an external-cavity diode laser (ECDL) emitting at 854 nm. The peculiar locking scheme, employing a direct-digital-synthesis (DDS) technique,⁹ makes the ECDL to be effectively phase-

^{a)} Author to whom correspondence should be addressed. Electronic mail: francesco.cappelli@ino.it.

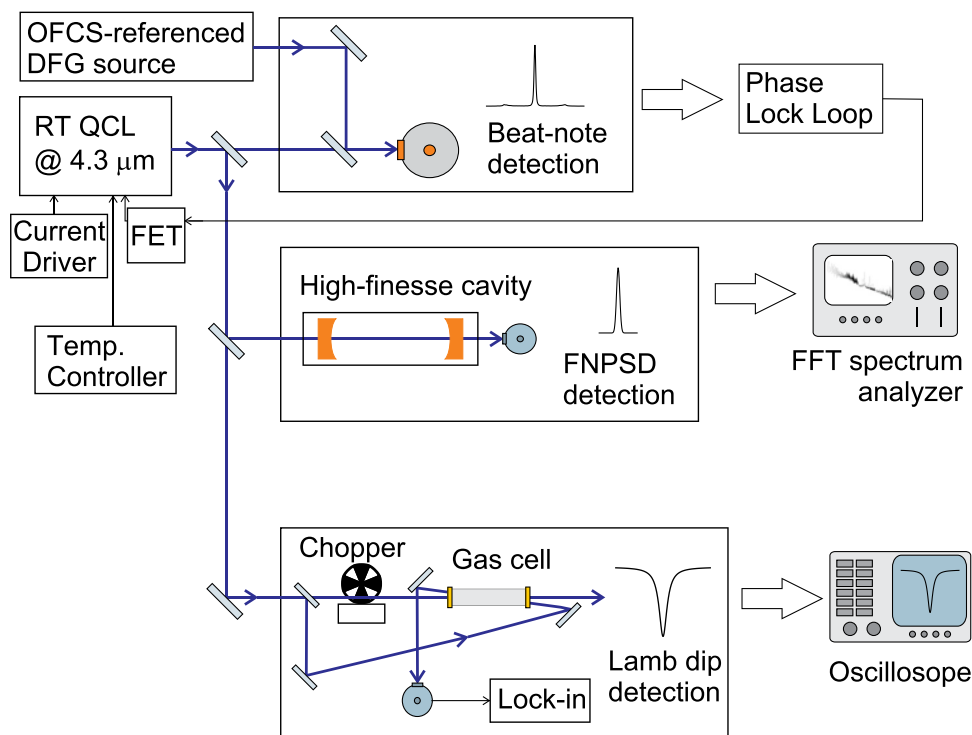


FIG. 1. Schematic of the experimental setup. There are three main parts: the beat-note detection between QCL and DFG for the phase-lock, the high-finesse cavity for FNPSD analysis, and the saturation spectroscopy signal detection for the absolute frequency measurement of the CO₂ transition. See Refs. 9 and 23 for more details.

locked to the Nd:YAG laser, while the OFCS just behaves as a transfer oscillator adding negligible phase-noise to the DFG radiation. As a consequence, the mid-IR radiation is referenced to the Cs frequency standard through the OFCS, but its linewidth is independent from that of the OFCS.

A schematic of the experimental setup is shown in Fig. 1. A small portion of the QCL beam, extracted by a beam-splitter, is used for the phase-lock: It is overlapped to the DFG source through a second beam splitter and sent to a 200-MHz-bandwidth HgCdTe detector. A 100-MHz beat-note is detected by using few μW of both QCL and DFG sources. The beat-note is processed by a home-made phase-detection electronics, which compares it with a 100-MHz local oscillator and provides the error signal for closing the phase-locked loop. A home-made proportional-integral-derivative (PID) electronics process the error signal and send it to the gate of a field effect transistor (FET) to fast control the QCL driving current. In Fig. 2, the beat-note acquired by FFT spectrum analyzer is shown: the width of the carrier frequency is limited by the instrumental resolution bandwidth (RBW), as expected from a beat-note between two phase-locked sources. According to what already reported elsewhere,^{19,22} the locking bandwidth is limited by the dependence of the QCL tuning rate on the modulation frequency. In fact, despite the completely different detector and electronics used, which are both much faster than those used in our previous work,²² we got the same 250-kHz locking bandwidth, as confirmed by the servo bumps in the beat-note. The phase-lock performance in terms of residual rms phase error is measured by using the fractional power η contained in the coherent part of the beat-note signal, i.e., in the carrier. By evaluating the ratio between the area under the central peak of the beat-note and the area under the whole beat-note spectrum (1.5 MHz wide), we obtain a phase-lock efficiency of $\eta = 73\%$. From $\eta = e^{-\phi_{\text{rms}}^2}$,²⁶ we measured a residual rms phase-noise of 0.56 rad.

The main portion of the QCL radiation is used for frequency-noise characterization and for spectroscopy. To the first purpose, the QCL beam is coupled to a high-finesse cavity, which works as frequency-to-amplitude converter, when its length is tuned in order to have a transmission corresponding to half the peak value. The cavity free spectral range is 150 MHz, and its finesse is about 9000 at $\lambda = 4.3 \mu\text{m}$, as measured with cavity-ring-down technique, leading to a mode FWHM of 18.8 kHz. The cavity output beam is detected by a second HgCdTe detector, and the resulting signal is processed by a FFT spectrum analyzer. In Fig. 3, the FNPSD of the phase-locked QCL, acquired by using the high-finesse cavity, is shown (trace b). The same cavity has been also used to measure the DFG FNPSD (trace c) and the QCL FNPSD when frequency-locked to a molecular line as in our previous work²² (trace d). Such an

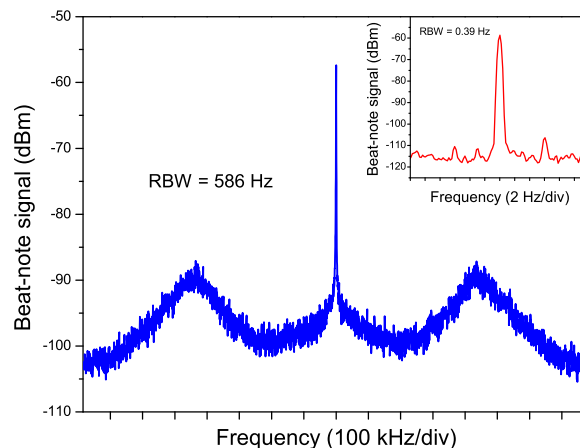


FIG. 2. Beat-note signal between the DFG radiation and the phase-locked QCL. The inset shows the same beat-note with a narrower span and resolution bandwidth. In both cases, the width of the peak (FWHM) is limited by the RBW of the spectrum analyzer.

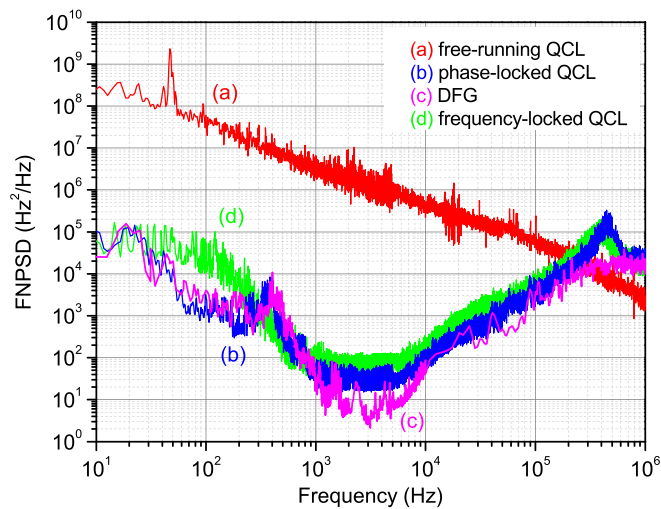


FIG. 3. QCL FNPSDs in free-running (trace a) and phase-locked (trace b) conditions, acquired by using a CO₂ line and the high-finesse cavity as frequency-to-amplitude converters, respectively. The cavity has been used also to measure the FNPSD of the DFG radiation (trace c) and that of the QCL, when it is frequency-locked to a molecular line as in our previous work²² (trace d).

independent converter allows for a fair comparison between the two basically different locking techniques. The plotted FNPSDs are compensated by the high-frequency cavity cut-off, due to the cavity ring-down rate ($f > 9.4$ kHz). The free-running QCL FNPSD (trace a), recorded by using the slope of the Doppler broadened CO₂ absorption line as converter, is shown. The comparison between free-running and phase-locked conditions confirms a locking bandwidth of 250 kHz, with a frequency noise reduction of about four orders of magnitude for frequencies up to 10 kHz. Moreover, the phase-locked-QCL FNPSD perfectly overlaps the DFG one, with only an excess noise above 200 kHz. If we compare the QCL FNPSD when phase/frequency locked to the DFG/molecular transition—traces b and d, respectively—they are almost coincident for Fourier frequencies above 1 kHz up to 450 kHz where a self-oscillation of both control loops is observed. This confirms that the locking bandwidth is limited by the laser modulation bandwidth. Nevertheless, a QCL linewidth narrower than 1 kHz (FWHM) on a time scale of 1 ms is retrieved in both cases by integrating the FNPSDs for frequencies above 1 kHz. As a consequence, we note that phase-locking the QCL does not improve laser narrowing with respect to frequency-locking. On the other hand, between 30 Hz and 1 kHz, the two curves show different trends: in this range, the phase-locked QCL FNPSD lies below that of the frequency-locked one, except for an evident noise peak centered at 400 Hz, which is also present in the DFG source (trace c). Apart from this peak, the comparison in this frequency range confirms a better control of the frequency jitter for the phase-locked QCL, overcoming the limits of the frequency-locked QCL set by the presence of a residual amplitude noise.²² For Fourier frequencies below 30 Hz, the high-finesse cavity is no more a good frequency-to-amplitude converter.

In order to confirm that the long-term frequency stability of the phase-locked QCL is limited by the OFCS stability (6×10^{-13} in 1 s), we have measured the Allan deviation of the DFG-QCL beat-note frequency. The result is 2.3 Hz at

1 s with a $\tau^{-1/2}$ trend up to 128 s, which is the last point used to compute the Allan deviation. Considering that the stability of this system is limited by the OFCS one, we can state that we have gained a factor of about 70 in terms of stability with respect to the frequency-locked QCL. Moreover, the accuracy of the phase-locked QCL is traceable to the primary frequency standard at the 2×10^{-12} level (140 Hz at 4.3 μ m). Therefore, we can conclude that the OFCS-DFG phase-locked QCL is a very suitable laser source for precision spectroscopy and metrological applications.

In order to test the spectral performances of the phase-locked QCL in terms of resolution, we performed saturated-absorption (SA) sub-Doppler spectroscopy of the CO₂ molecule around 4.3 μ m in a single-pass cell. The SA setup, depicted schematically in Fig. 1, uses about 5 mW of power of the QCL in a standard pump-probe configuration. Thanks to the absolute reference, it is possible to measure the absolute center frequency of the P(29) molecular transition of the (01¹1 – 01¹0) ro-vibrational band of CO₂, the same that was investigated by polarization-spectroscopy technique in our previous work.²² In the SA scheme, the Lamb dip at the center of the Doppler-broadened molecular line is detected (Fig. 1). An optical chopper on the pump beam, combined with lock-in detection, allows to automatically cancel out the Doppler background and to retrieve the Lorentzian Lamb-dip profile with an increased signal-to-noise ratio. The frequency of the phase-locked QCL is scanned across the Lamb dip by tuning the frequency of the DFG source. The link to the OFCS automatically provides each scan with the absolute frequency scale. A typical acquisition is shown in Fig. 4 (inset), together with the Lorentzian fit and the corresponding residuals.

Thanks to the high precision achieved by our setup, we can perform a series of acquisitions by varying the pressure of the CO₂ gas in a very small range (from 2 to 27 Pa, Fig. 4). A linear dependence of the line center on pressure

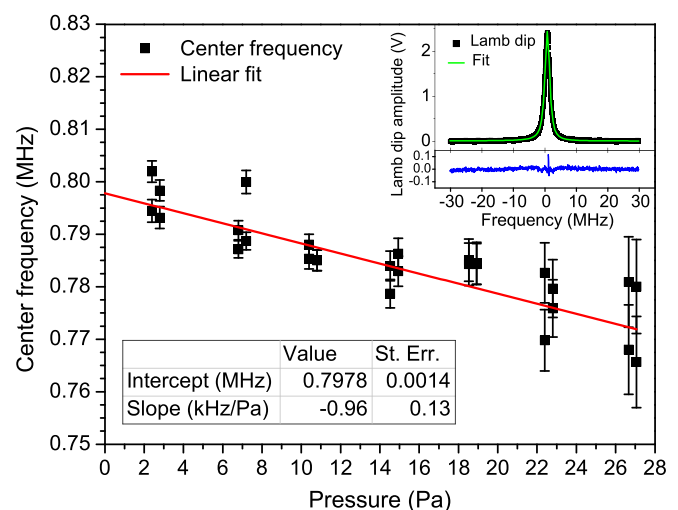


FIG. 4. Dependence of the center of the Lamb dip of the CO₂ (01¹1 – 01¹0) P(29) transition on pressure, with the corresponding linear fit. For clarity, the constant value of 69 297 478 MHz has been subtracted from the absolute frequency values. Inset: example of a single Lamb-dip acquisition (black squares). Experimental conditions: lock-in amplifier time constant 10 ms, chopper frequency 616 Hz, frequency scan with 60-MHz span, and 50 kHz steps. The fit with a Voigt function (green line) and the residuals are also plotted.

(pressure shift) of (-0.96 ± 0.13) kHz/Pa has been measured from this slope. The extrapolated value at $P = 0$, $\nu_0 = (69297478.7978 \pm 0.0014)$ MHz is the absolute frequency of the CO₂ transition corrected by systematic pressure shift. This value is in agreement with that measured for the QCL frequency-locked to this CO₂ transition²² with an uncertainty improved by almost a factor of 20.

In conclusion, we have demonstrated the phase-locking of a mid-IR QCL to an OFCS-referenced DFG source. The 250-kHz bandwidth with a residual rms phase-noise of 0.56 rad leads to a subkilohertz-linewidth QCL radiation. The QCL frequency stability is 6×10^{-13} in 1 s with an absolute traceability accurate in 2×10^{-12} , both limited by the Rb-GPS-disciplined 10-MHz quartz oscillator reference of the OFCS. Spectroscopic application is demonstrated by absolute frequency measurements of a CO₂ transition, with a 2×10^{-11} precision.

This work was financially supported by Ente Cassa di Risparmio di Firenze, by the Extreme Light Infrastructure (ELI) European project, by the Laserlab-Europe Consortium in the ALADIN project framework, and by the Progetto Operativo Nazionale (PON) PON01_01525 Monitoraggio Innovativo per le Coste e l'Ambiente Marino (MONICA) funded by Italian Ministry of Education, University and Research (MIUR).

¹S. A. Diddams, D. J. Jones, J. Ye, S. T. Cundiff, J. L. Hall, J. K. Ranka, R. S. Windeler, R. Holzwarth, T. Udem, and T. W. Hänsch, *Phys. Rev. Lett.* **84**, 5102 (2000).

²A. Schliesser, N. Picqué, and T. W. Hänsch, *Nat. Photonics* **6**, 440 (2012).

³M. Zimmermann, C. Gohle, R. Holzwarth, T. Udem, and T. W. Hänsch, *Opt. Lett.* **29**, 310 (2004).

⁴C. Erny, K. Moutzouris, J. Biegert, D. Kühle, F. Adler, A. Leitenstorfer, and U. Keller, *Opt. Lett.* **32**, 1138 (2007).

⁵E. Baumann, F. R. Giorgetta, W. C. Swann, A. M. Zolot, I. R. Coddington, and N. R. Newbury, *Phys. Rev. A* **84**, 062513 (2011).

⁶A. Ruehl, A. Gambetta, I. Hartl, M. E. Fermann, K. S. E. Eikema, and M. Marangoni, *Opt. Lett.* **37**, 2232 (2012).

⁷F. Adler, K. C. Cossel, M. J. Thorpe, I. Hartl, M. E. Fermann, and J. Ye, *Opt. Lett.* **34**, 1330 (2009).

⁸N. Leindecker, A. Marandi, R. L. Byer, and K. L. Vodopyanov, *Opt. Express* **19**, 6296 (2011).

⁹I. Galli, S. Bartalini, P. Cancio, G. Giusfredi, D. Mazzotti, and P. De Natale, *Opt. Express* **17**, 9582 (2009).

¹⁰I. Galli, S. Bartalini, S. Borri, P. Cancio, G. Giusfredi, D. Mazzotti, and P. De Natale, *Opt. Lett.* **35**, 3616 (2010).

¹¹M. H. Dunn and M. Ebrahimzadeh, *Science* **286**, 1513 (1999).

¹²I. Galli, S. Bartalini, S. Borri, P. Cancio, D. Mazzotti, P. De Natale, and G. Giusfredi, *Phys. Rev. Lett.* **107**, 270802 (2011).

¹³G. Giusfredi, S. Bartalini, S. Borri, P. Cancio, I. Galli, D. Mazzotti, and P. De Natale, *Phys. Rev. Lett.* **104**, 110801 (2010).

¹⁴I. Ricciardi, E. D. Tommasi, P. Maddaloni, S. Mosca, A. Rocco, J.-J. Zondy, M. D. Rosa, and P. De Natale, *Opt. Express* **20**, 9178 (2012).

¹⁵J. Faist, F. Capasso, D. L. Sivco, C. Sirtori, A. L. Hutchinson, and A. Y. Cho, *Science* **264**, 553 (1994).

¹⁶R. Maulini, I. Dunayevskiy, A. Lyakh, A. Tsekoun, C. K. N. Patel, L. Diehl, C. Pflugl, and F. Capasso, *Electron. Lett.* **45**, 107 (2009).

¹⁷Q. Y. Lu, Y. Bai, N. Bandyopadhyay, S. Slivken, and M. Razeghi, *Appl. Phys. Lett.* **98**, 181106 (2011).

¹⁸M. Yamanishi, T. Edamura, K. Fujita, N. Akikusa, and H. Kan, *IEEE J. Quantum Electron.* **44**, 12 (2008).

¹⁹L. Tombez, J. D. Francesco, S. Schilt, G. D. Domenico, J. Faist, P. Thomann, and D. Hofstetter, *Opt. Lett.* **36**, 3109 (2011).

²⁰S. Bartalini, S. Borri, I. Galli, G. Giusfredi, D. Mazzotti, T. Edamura, N. Akikusa, M. Yamanishi, and P. De Natale, *Opt. Express* **19**, 17996 (2011).

²¹M. S. Vitiello, L. Consolino, S. Bartalini, A. Taschin, A. Tredicucci, M. Inguscio, and P. De Natale, *Nat. Photonics* **6**, 525 (2012).

²²F. Cappelli, I. Galli, S. Borri, G. Giusfredi, P. Cancio, D. Mazzotti, A. Montori, N. Akikusa, M. Yamanishi, S. Bartalini, and P. De Natale, *Opt. Lett.* **37**, 4811 (2012).

²³S. Borri, I. Galli, F. Cappelli, A. Bismuto, S. Bartalini, P. Cancio, G. Giusfredi, D. Mazzotti, J. Faist, and P. De Natale, *Opt. Lett.* **37**, 1011 (2012).

²⁴S. Barbieri, P. Gellie, G. Santarelli, L. Ding, W. Maineult, C. Sirtori, R. Colombelli, H. Beere, and D. Ritchie, *Nat. Photonics* **4**, 636 (2010).

²⁵A. Mills, D. Gatti, J. Jiang, C. Mohr, W. Mefford, L. Gianfrani, M. Fermann, I. Hartl, and M. Marangoni, *Opt. Lett.* **37**, 4083 (2012).

²⁶M. Prevedelli, T. Freearge, and T. W. Hänsch, *Appl. Phys. B* **60**, 73 (1995).